Leishmania major Pteridine Reductase 1 Belongs to the Short Chain Dehydrogenase Family: Stereochemical and Kinetic Evidence†

James Luba,‡,§ Bakela Nare,||,⊥ Po-Huang Liang,# Karen S. Anderson,# Stephen M. Beverley,||,@ and Larry W. Hardy*,‡

Department of Pharmacology and Molecular Toxicology, University of Massachusetts Medical Center, 55 Lake Avenue North, Worcester, Massachusetts 01605, Department of Biological Chemistry and Molecular Pharmacology, Harvard Medical School, Boston, Massachusetts 02115, and Department of Pharmacology, 333 Cedar Street, Yale University School of Medicine, New Haven, Connecticut 06520-8066

Received October 30, 1997; Revised Manuscript Received January 5, 1998

ABSTRACT: Pteridine reductase 1 (PTR1) is a novel broad spectrum enzyme of pterin and folate metabolism in the protozoan parasite *Leishmania*. Overexpression of PTR1 confers methotrexate resistance to these protozoa, arising from the enzyme's ability to reduce dihydrofolate and its relative insensitivity to methotrexate. The kinetic mechanism and stereochemical course for the catalyzed reaction confirm PTR1's membership within the short chain dehydrogenase/reductase (SDR) family. With folate as a substrate, PTR1 catalyzes two rounds of reduction, yielding 5,6,7,8-tetrahydrofolate and oxidizing 2 equiv of NADPH. Dihydrofolate accumulates transiently during folate reduction and is both a substrate and an inhibitor of PTR1. PTR1 transfers the *pro-S* hydride of NADPH to carbon 6 on the *si* face of dihydrofolate, producing the same stereoisomer of THF as does dihydrofolate reductase. Product inhibition and isotope partitioning studies support an ordered ternary complex mechanism, with NADPH binding first and $NADP^+$ dissociating after the reduced pteridine. Identical kinetic mechanisms and NAD(P)H hydride chirality preferences are seen with other SDRs. An observed tritium effect upon *V*/*K* for reduction of dihydrofolate arising from isotopic substitution of the transferred hydride was suppressed at a high concentration of dihydrofolate, consistent with a steady-state ordered kinetic mechanism. Interestingly, half of the binary enzyme−NADPH complex appears to be incapable of rapid turnover. Fluorescence quenching results also indicate the existence of a nonproductive binary enzyme−dihydrofolate complex. The nonproductive complexes observed between PTR1 and its substrates are unique among members of the SDR family and may provide leads for developing antileishmanial therapeutics.

Pteridine reductase 1 (PTR1)[1] is a novel enzyme (tentative EC number 1.1.1.253) of pterin metabolism in the trypanosomatid parasite *Leishmania*. Isolation of the gene for PTR1 was aided by its amplification in some methotrexate-resistant strains of the protozoan (*1*−*3*). Recent studies indicate that a major physiological role for PTR1 in *Leishmania* is the salvage of oxidized pterins and folates, for which this organism is auxotrophic (*4*−*6*). PTR1 is likely responsible for the failure of anti-folate therapeutic strategies targeted against dihydrofolate reductase (DHFR), since it catalyzes the same reaction as DHFR and is much less susceptible to inhibition by several clinically useful DHFR inhibitors (*7*, *8*). A detailed understanding of the mechanism of catalysis by PTR1 is therefore a desirable goal. This understanding will assist in the development of effective inhibitors of this enzyme, which may render *Leishmania* DHFR vulnerable as a drug target in this human parasite.

Analysis of the amino acid sequence of PTR1 led to suggestions (*2*, *3*) that the protein belongs to a large group of oxidoreductases, which includes the aldoketoreductases [AKRs (*9*)] and the short chain dehydrogenases/reductases [SDRs (*10*)]. Because of the large evolutionary distance encompassed by both the AKR and SDR families, unambiguous assignment to one family or the other was not possible on the basis of amino acid sequence similarities alone. For this assignment, stereochemical and kinetic information about the reaction catalyzed by PTR1 was also required. Although both families of oxidoreductases utilize nicotinamide nucleotides as substrates and generally require no metal cofactors, AKRs and SDRs have distinct protein

† Supported by grants from the NIH (Grant GMS 43023 to L.W.H. and Grant AI 21903 to S.M.B.), a postdoctoral fellowship to B.N. from the Charles King Trust, and an American Heart Association Established Investigator Award to L.W.H.

* To whom correspondence should be addressed. Telephone: (508) 856-4900. Fax: (508) 856-4289. E-mail: larry.hardy@ummed.edu.

‡ University of Massachusetts Medical Center.

§ Current address: Department of Biochemistry, Wake Forest University Medical Center, Medical Center Boulevard, Winston-Salem, North Carolina 27157-1016.

|| Harvard Medical School.

⊥ Current address: Merck Research Laboratories, Merck & Co., Inc., P.O. Box 2000, R80Y-260, Rahway, New Jersey 07065-0900.

Yale University.

@ Current address: Department of Molecular Microbiology, Washington University School of Medicine, 760 McDonnell Science Bldg., 660 S. Euclid Ave., St. Louis, Missouri 63110-1093.

[1] Abbreviations: AKR, aldoketo reductase; DHF, 7,8-dihydrofolate; DHFR, dihydrofolate reductase; DHPR, dihydropteridine reductase; dTMP, thymidylate; dUMP, 2′-deoxyuridylate; ^{D}V, deuterium isotope effect on V_{max}; $^{D}(V/K)$, deuterium isotope effect on V_{max}/K_M; PTR1, pteridine reductase 1; SDR, short chain dehydrogenase/reductase; THF, 5,6,7,8-tetrahydrofolate; 5dTHF, 5-deaza-5,6,7,8-tetrahydrofolate; TS, thymidylate synthase; $^{T}(V/K)$, tritium isotope effect on *V*/*K*.

S0006-2960(97)02693-7 CCC: $15.00
Published on Web 03/03/1998

folds, differing stereochemical courses, and probably different catalytic mechanisms. The SDRs are B-side dehydrogenases, and the AKRs are A-side dehydrogenases. The data presented here demonstrate that PTR1 has the stereochemical course and kinetic characteristics typical of members of the SDR family. More than 50 members of the SDR family have been identified to date (reviewed in ref *10*). The proteins are frequently homodimers or homotetramers, possess a unique N-terminal $\beta-\alpha-\beta$ unit which is involved in the binding of NADH or NADPH, and typically have a Tyr-$(Xaa)_3$-Lys motif which has been implicated in catalysis. PTR1 is a homotetramer (*5*, *6*), with two Tyr-$(Xaa)_3$-Lys sequences and an N-terminal sequence which is significantly similar to SDR sequences corresponding to the $\beta-\alpha-\beta$ unit.

One of the most well studied members of the SDR family is the mammalian enzyme, dihydropteridine reductase (DHPR). The three-dimensional structures of DHPR (*11*) and several other SDRs [3α,20β-hydroxysteroid dehydrogenase (*12*), carbonyl reductase (*13*), and 7α-hydroxysteroid dehydrogenase (*14*)] have been determined by X-ray crystallographic methods. The structures reveal a conserved core, with significant structural diversity arising from the highly variant C-terminal sequences of these proteins. A key feature, based upon both kinetic and crystallographic evidence, is that the binding of the nicotinamide cofactor must occur for creation of a competent enzyme (*15*).

A strain of *Escherichia coli* engineered to overproduce recombinant *Leishmania major* PTR1 has provided an abundant supply of the enzyme (*4*). Homogeneous PTR1 purified from this bacterial strain behaves in the same manner as the enzyme isolated from the native protozoan (*5*), and was employed in the studies described here.

MATERIALS AND METHODS

Materials. (4*S*)-[^{3}H]NADPH and (4*R*)-[^{3}H]NADPH were generated by published methods using, respectively, glucose-6-phosphate dehydrogenase (*16*) and malic enzyme (*17*). [1-^{3}H]Glucose 6-phosphate was generated in situ from [1-^{3}H]-glucose (from Moravek Biochemicals) using hexokinase. (4*S*)-[^{2}H]NADPH was generated by the same methods as (4*S*)-[^{3}H]NADPH, except that [1-^{2}H]glucose 6-phosphate was generated in situ from [1-^{2}H]glucose. [2-^{3}H]Malic acid was generated by reduction of oxaloacetate with [^{3}H]$NaBH_4$ according to a published procedure (*18*).

The [*adenosine*-^{14}C]NADPH for isotope partitioning experiments was generated as follows. NAD^+ kinase (Sigma) was used to catalyze the phosphorylation of [*adenosine*-^{14}C]-NAD^+ (DuPont NEN) by ATP, according to a published procedure (*19*). The [*adenosine*-^{14}C]$NADP^+$ was reduced using glucose 6-phosphate and glucose-6-phosphate dehydrogenase and purified by HPLC (*20*). The purities of $NADP^+$, NADPH, folate, dihydrofolate (DHF), and methotrexate were routinely confirmed to be >95% by HPLC. Folate was recrystallized from ethanol/water prior to use. DHF was either synthesized from folate by dithionite reduction (*21*) or purchased from Schircks Laboratories (Jona, Switzerland). 5-Deaza-5,6,7,8-tetrahydrofolate (5dTHF) was a gift from C. J. Shih of Eli Lilly Research Laboratories. Methotrexate was purchased from Schircks or Sigma. [3′,5′,7,9-^{3}H]Folic acid was from Moravek. The isolations of homogeneous recombinant *L. major* PTR1 (5), *E. coli* thymidylate synthase (*22*), and *E. coli* DHFR (*23*) were carried out using methods previously described.

HPLC Methods. Large scale separation of $NADP^+$ and NADPH was conducted on a semipreparative Exasil C18 column (250 × 10 mm) essentially as described by Gready and co-workers (*20*). For smaller quantities or for analytical purposes, $NADP^+$ and NADPH were isolated by reverse phase HPLC on a 250 × 4.6 mm C18 column eluted at 1 mL/min with a mobile phase consisting of 5 mM tetrabutylammonium sulfate, 5 mM potassium phosphate (pH 7.5), and 28.5% methanol (HPLC buffer A). This HPLC system was also used for analysis of the folates following isotope trapping experiments. Nonradioactive $NADP^+$/NADPH and folates were detected by monitoring UV absorbance at 260 and 295 nm, respectively, using a Waters model 481 LC spectrophotometer linked to an autointegrator (Waters 740 data module). The retention times during analytical runs were 12 and 35 min for $NADP^+$ and NADPH, respectively. The radiolabeled nucleotides produced by the coupled action of PTR1 and thymidylate synthase (TS) were separated by reverse phase C18 HPLC using a mobile phase of 5 mM tetrabutylammonium sulfate, 5 mM potassium phosphate (pH 7.5), and 8% methanol (HPLC buffer B). Proteins were removed from most samples prior to HPLC by passage through a Centricon-10 unit.

The substrates and products from the rapid chemical quench experiments were quantified by HPLC using a radioactivity flow detector. The HPLC separation was performed using a BDS-Hypersil C18 reverse phase column (250 × 4.6 mm, Keystone Scientific, Bellefonte, PA) with a flow rate of 1 mL/min. The HPLC effluent from the column was mixed with liquid scintillation cocktail (Monoflow V, National Diagnostics) at flow rate of 4 mL/min. Radioactivity was monitored continuously using a Flo-One radioactivity flow detector (Packard Instruments, Downers Grove, IL). The analysis system was automated by the use of a Waters 712B WISP (Milford, MA) autosampler.

Stereochemical Course. The stereochemistry at carbon 6 of the THF produced by PTR1-catalyzed reduction of DHF was determined by coupling the reaction to TS, an enzyme known to require the 6*R* isomer of 5,10-methylene-THF (*24*−*26*). The reaction was conducted under argon in a solution containing 20 mM sodium 4-(2-hydroxyethyl)-1-piperazine-ethanesulfonate (pH 7), 0.4 mM [2-^{14}C]deoxyuridylate (dUMP) (45 Ci/mol), 0.5 mM (4*S*)-[^{3}H]NADPH (680 Ci/mol), 0.2 mM folate, and 1 mM formaldehyde. (This concentration of formaldehyde was shown in a separate experiment to have no effect on the activity of either PTR1 or TS.) The reaction was initiated by addition of 2.8 μM PTR1 and 3.3 μM TS. Samples of 0.1 mL were removed from the reaction mixture at 15 min intervals and frozen on dry ice. After samples were thawed and treated to remove proteins, the radiolabeled dUMP and thymidylate (dTMP) produced were separated by HPLC and quantitated by liquid scintillation counting.

Spectrophotometric Methods and Rate Assays. The concentrations of PTR1 determined using the molar absorbance at 280 nm calculated from Tyr and Trp content (26.8 mM^{-1} cm^{-1}) were identical to those measured by the Coomassie dye-binding method (*27*). The spectrophotometric rate assay for NADPH-dependent reduction of pteridines catalyzed by PTR1 was performed at pH 7.0 and 30 °C. Although the

pH optimum for the reduction of folate by PTR1 is 6.0, measurements were carried out at pH 7.0 to decrease the rate of nonenzymatic oxidation of NADPH. The assay buffer and substrate solutions were made dust-free by passage through 0.45 μm filters, to minimize fluctuations in the initial velocity measurements. The assays were initiated by the addition of enzyme, and the rate was measured for 15 s. Less than 20% of the substrates were consumed during assays, except those carried out at the lowest substrate concentrations. Data were fit to eqs 1−8 using the program Kaleidagraph (Synergy Software).

Initial velocities (v_i) were measured at several fixed concentrations of folate (0.75, 1, 1.5, 3, or 6 μM) while NADPH was varied from 2 to 80 μM. Because the order of substrate binding was not known, initial velocities were also measured at several fixed concentrations of NADPH (5, 10, 20, or 40 μM) while folate was varied from 0.75 to 16 μM. The concentration of PTR1 used for these measurements was 0.33 or 0.66 μM. Apparent values of the kinetic parameters (V_{max}^{app} and K_M^{app} for each varied substrate, S) were calculated by nonlinear least-squares regression of the data (at the fixed concentrations of the second substrate) onto

$$v_i = \frac{V_{max}^{app}[S]}{K_M^{app} + [S]} \quad (1)$$

To determine if the PTR1-catalyzed reaction proceeds through a substituted or ternary complex mechanism, the appropriate double-reciprocal plots were examined (*28*). All the initial velocity measurements were pooled, and V_{max}, the K_M for NADPH (K_{MN}), the K_M for folate (K_{MF}), and the K_d for NADPH (K_{iN}) were determined from the re-plots of intercepts ([folate]/V_{max}^{app}) and slopes ([folate]K_M^{app}/V_{max}^{app}) as functions of [folate] using the relationships (*29*)

$$[folate]/V_{max}^{app} = \frac{K_{MF}}{V_{max}} + \frac{[folate]}{V_{max}} \quad (2)$$

and

$$[folate]K_M^{app}/V_{max}^{app} = \frac{K_{iN}K_{MF}}{V_{max}} + \frac{K_{MN}[folate]}{V_{max}} \quad (3)$$

To determine the order of substrate binding, the patterns of inhibition by $NADP^+$ and by the stable product analogue 5dTHF were determined with respect to folate and NADPH. For measurements of v_i as a function of NADPH concentration, folate was fixed at 30 μM, $NADP^+$ was fixed at 2.5, 5, or 10 μM, and 5dTHF was fixed at 20, 40, or 80 μM. For measurements of v_i as a function of folate concentration, NADPH was fixed at 90 μM, $NADP^+$ was fixed at 1, 2.5, or 5 μM, and 5dTHF was fixed at 10, 20, or 40 μM. V^{app} and K_M^{app} for folate and NADPH were calculated at each concentration of $NADP^+$ and 5dTHF. Data that showed evidence of competitive, noncompetitive, and uncompetitive inhibition in double-reciprocal plots (*30*) were analyzed using eqs 4−6, respectively,

$$v_i = \frac{V_o^{app}S}{K_o^{app}(1 + I/K_i) + S} \quad (4)$$

$$v_i = \frac{V_o^{app}S/(1 + I/K_i)}{K_o^{app} + S} \quad (5)$$

$$v_i = \frac{V_o^{app}S/(1 + I/K_i)}{K_o^{app}/(1 + I/K_i) + S} \quad (6)$$

where S represents the concentration of the varied substrate, I is the concentration of inhibitor, V_o^{app} is the apparent V_{max} in the absence of inhibitor, K_o^{app} is the apparent K_M in the absence of inhibitor, and K_i is the inhibition constant.

Fluorescence Measurements of Ligand Binding. The binding of NADPH to PTR1 was monitored by fluorescence energy transfer from the protein to NADPH, using excitation at a λ_{ex} of 295 nm and emission at a λ_{em} of 450 nm. The binding of DHF to PTR1 was measured by monitoring the quenching of the fluorescence emission of the protein, using a λ_{ex} of 290 nm and a λ_{em} of 340 nm. All fluorescence measurements were carried out at 30 °C, at pH 6, using a Farrand MK2 fluorescence spectrometer, with 5 μM PTR1 unless otherwise noted. The decreased intensity of PTR1's fluorescence emission at 340 nm which occurs upon addition of DHF was corrected for a small amount of absorbance at this wavelength by DHF. This correction was done by measuring the decreased intensity of fluorescence emission of a 7.5 μM solution of tryptophan in the same buffer. In the concentration range of DHF used (0−48 μM), the decrease due to absorbance was linear, with a 0.18% decrease of the fluorescence signal per micromolar unit of DHF.

The quantitative analysis of the NADPH fluorescence by 0.5 μM PTR1 was similar to that described by Janin et al. (*31*) for binding of NADPH to homoserine dehydrogenase. Briefly, the data above 5 μM NADPH increased linearly with NADPH concentration, and the values below this approached this line asymptotically. Differences between the extended line and the observed fluorescence arising from the NADPH−PTR1 complex from 0.05 to 0.95 μM NADPH were used to calculate the fraction of PTR1 bound to NADPH (Y). A plot of $(1 - Y)^{-1}$ versus $[NADPH]_{total}/Y$ yielded a line of slope K_d^{-1}.

The quenching of PTR1 fluorescence by DHF was analyzed using the relationship

$$\Delta F = F_0 - F = F_0\left(\frac{S}{K_d + S}\right) \quad (7)$$

where F_0 and F are the observed fluorescence intensities in the absence and presence of ligand, respectively, K_d is the apparent dissociation constant, and S is the concentration of dihydrofolate.

Isotope Partitioning. To determine if the binary PTR1−NADPH complex was productive, the complex was preformed by preparing a solution containing 20 or 40 μM PTR1 and 20 μM [*adenosine*-^{14}C]NADPH (1.5 Ci/mol). This solution was then rapidly mixed with an equal volume of 80 μM DHF and 2 mM NADPH (the chase). The mixture was incubated at ambient temperature (ca. 22 °C) for 12 s (sufficient for a single turnover), and the reaction was quenched with 40 μM methotrexate. $NADP^+$ was separated from NADPH by HPLC, and the HPLC fractions were analyzed by liquid scintillation counting. Controls for these experiments included reactions in the absence of PTR1, in

the absence of the nonradiolabeled NADPH chase, and with the [^{14}C]NADPH added to the chase instead of being prebound to the enzyme.

To determine if the binary complex between PTR1 and DHF was productive, 20 μM PTR1 was incubated with 20 μM [^{3}H]DHF (3 Ci/mol) to form the complex. After this solution was mixed with equal volume of 100 μM NADPH and 2 mM DHF and incubated for 12 s, an analysis similar to that described above was done, with the appropriate HPLC system to separate DHF and THF. To determine whether the binary complex between PTR1 and folate was productive, a solution containing 20 μM PTR1 and 20 μM [^{3}H]folate (500 Ci/mol) was rapidly mixed with an equal volume of 100 μM NADPH and 2 mM folate and analyzed as described above. Controls were included to demonstrate that radiolabeled substrates were capable of conversion to products in the absence of a chase by unlabeled substrates and to verify the stability of the radiolabeled products during the analysis.

Kinetic Isotope Effects. The deuterium isotope effect on V_{max}, ^{D}V, and on V_{max}/K_M, $^{D}(V/K)$, were measured using the spectrophotometric assay. ^{D}V and $^{D}(V/K)$ are defined in the nomenclature of Northrop (*32*). To minimize errors arising from slight variations in enzyme activity or assay conditions, data were collected at varying [4-^{1}H]NADPH and (4*S*)-[^{2}H]-NADPH concentrations on the same day, using 30 μM folate. The data from the 4-deuterated cofactor was fit to

$$[[^2\text{H}]\text{NADPH}](v_i)^{-1} = \frac{[[^2\text{H}]\text{NADPH}]}{V_{max,D}} + \frac{K_{MN,D}}{V_{max,D}} \quad (8)$$

where $V_{max,D}$ and $K_{MN,D}$ were, respectively, the values for V_{max} and K_{MN} measured with (4*S*)-[^{2}H]NADPH. The kinetic parameters for [4-^{1}H]NADPH were obtained similarly.

The instability of the product THF under the assay conditions made it challenging to measure the tritium effect on V_{max}/K_{MN} [$^{T}(V/K)$] arising from the tritium substitution of the *pro-S* hydrogen at C4 of NADPH. In our initial attempts, the fraction of NADPH consumed, *f* (measured either by A_{340} or by liquid scintillation counting of [^{14}C]-NADPH and [^{14}C]NADP$^+$ following HPLC separation, or by alcohol dehydrogenase assay), could not be quantitated with sufficient reproducibility to give the necessary precision. This was likely the result of the nonenzymatic oxidation of THF to DHF, resulting in additional rounds of PTR1-catalyzed NADPH oxidation, slight losses of stoichiometry at longer reaction times, and variability in the apparent values of *f*. The possible regeneration of DHF also caused uncertainty about the exact DHF concentration, a critical variable in this experiment. These problems were circumvented by coupling the reduction of DHF by PTR1 with the methylation of dUMP by TS, using enough TS to ensure that the resulting isotope effects were due only to the PTR1-catalyzed reaction. Measurements of the production of the stable product dTMP allowed valid estimates of *f* to be made with accuracy and precision. Thus, values of $^{T}(V/K)$ could be calculated from the observed changes in the specific activity of residual (4*S*)-[^{3}H]NADPH and in the ratio of [2-^{14}C]dTMP to the sum of [2-^{14}C]dTMP and [2-^{14}C]dUMP produced by the coupled system. The product recycling method which we employed had an additional advantage. It ensured that the concentration of DHF remained constant at all times, because any THF formed was immediately converted to its 5,10-methylene derivative and oxidized by TS back to DHF. Hence, it was unnecessary to make multiple additions of the substrate being reduced to maintain a constant concentration.

Measurements were made at 0.5 and 60 μM DHF. All reactions were carried out at 30 °C in 25 mM Tris (pH 7.5) under N_2, and the mixtures contained 300 μM (4*S*)-[^{3}H]-NADPH (ca. 15 Ci/mol), 300 μM dUMP (3.3 Ci/mol), 2 mM formaldehyde, 1.5 μM PTR1, and 1.6 μM TS in a volume of 2 mL. Using these conditions in separate control experiments, TS turnover was determined to be 10 000 times faster than PTR1 turnover. The samples were reacted for 1.5 h for the measurements at 0.5 μM DHF or for 10−15 min for the measurements at 60 μM DHF. To quench each reaction, 0.66 mL of CCl_4 was added to the 2 mL sample with rapid mixing to denature and inactivate the enzymes. The organic and aqueous phases were separated by spinning the mixture in a clinical centrifuge, and the aqueous layer was removed with a Pasteur pipet.

To allow a determination of the initial specific activity of (4*S*)-[^{3}H]NADPH prior to the addition of enzymes, the absorbance at 340 nm of samples of the reaction solution (diluted 20-fold into HPLC buffer A) was measured seven times, and the radioactivity in the diluted samples was quantitated by counting in Ready Safe scintillation fluid to 2σ values of <0.2%.

The final specific activity of (4*S*)-[^{3}H]NADPH was measured by purifying the remaining NADPH from the reaction mixture by HPLC, using the semipreparative column described above with a mobile phase of HPLC buffer A. Fractions containing an A_{260}/A_{340} ratio of <2.4 were pooled. The absorbance at 340 nm of the pool was measured seven times, and seven samples were counted for ^{3}H as described above.

The fraction of NADPH consumed was measured by quantitating the conversion of [2-^{14}C]dUMP to [2-^{14}C]dTMP. dUMP and dTMP were purified from the quenched reaction mixture by HPLC as described above. Fractions containing either dUMP or dTMP were mixed with 5 mL of Ready Safe scintillation fluid and counted for ^{14}C to 2σ values of <0.2%. The fraction of conversion was calculated from the relationship

$$f = ([\text{NADPH}]_0/[\text{dUMP}]_0) \times \text{dpmT}/(\text{dpmT} + \text{dpmU}) \quad (9)$$

where dpmT represents the total ^{14}C disintegrations per minute (dpm) in dTMP, dpmU represents the total ^{14}C dpm in dUMP, $[\text{NADPH}]_0$ represents the initial concentration of NADPH, and $[\text{dUMP}]_0$ represents the initial concentration of dUMP. The reactions at 60 μM DHF were allowed to proceed to fractional conversion of 0.6−0.8, to allow for larger values of R_s/R_o (defined below). This, in turn, allowed for more precise estimates of the near unity $^{T}(V/K)$ values.

The tritium effect on *V*/*K* was calculated using the relationship (*33*)

$$^{T}(V/K) = \frac{\log(1-f)}{\log[(1-f)(R_s/R_o)]} \quad (10)$$

where *f* is the fraction of NADPH converted to NADP$^+$ (from

eq 9), R_0 is the initial specific activity of NADPH, and R_s is the specific activity of NADPH at fractional conversion *f*.

Rapid Chemical Quench Experiments. All measurements were carried out using a Kintek RFQ-3 rapid chemical quench apparatus (Kintek Instruments, State College, PA). Each reaction was initiated by mixing 15 μL of PTR1 (73 or 160 μM) and 1 mM NADPH with an equal volume of radiolabeled substrate (either 20 μM [^{3}H]folate or [^{3}H]DHF). The solutions were rapidly mixed and then aged (0.2−40 s for folate or 0.005−60 s for DHF). The concentrations of enzyme and substrates cited below in the discussion of the pre-steady state kinetic results and in the legend of Figure 10 are those after mixing and during the enzymatic reaction. The enzyme reactions were terminated by quenching with 67 μL of 0.78 N KOH to give a final concentration of 0.54 N KOH. The basic quench solution contained 10% sodium ascorbate (pH 12.7) to prevent THF degradation after reactions were terminated. The quenched reaction solution was directly collected into an argon-purged vial for a Waters WISP autosampler, vortexed, and analyzed by HPLC in combination with radioactivity flow detection. The substrates and products were quantified by HPLC as described above. To ensure that the base was quenching the enzymatic reaction, a control was included with each experiment to ensure that catalysis was being terminated. This involved adding the substrate to a premixed solution of base and enzyme. Samples were collected in vials containing an argon atmosphere to protect against oxidation during subsequent analysis. Control experiments were also carried out to establish the stability of the radiolabeled substrates and products under the quench conditions employed.

RESULTS AND DISCUSSION

Stereochemical Course. The conversions of DHF and of folate to THF by PTR1 were accompanied, respectively, by the stoichiometric oxidation of 1 and 2 equiv of NADPH to $NADP^+$. The reduction of folate or DHF by (4*S*)-[^{3}H]-NADPH catalyzed by PTR1 yielded nonradioactive $NADP^+$. In contrast, tritium was retained by $NADP^+$ when (4*R*)-[^{3}H]-NADPH was used. The opposite results were observed when (4*R*)- and (4*S*)-[^{3}H]NADPH were used for the reduction of DHF catalyzed by *E. coli* DHFR. The latter result was consistent with the previously described chirality preference for DHFR (*34*, *35*). Thus, PTR1 transfers the 4*S* prochiral hydrogen from NADPH.

It was important to determine whether carbon or nitrogen is the hydrogen acceptor during PTR1-catalyzed transfer of a hydride equivalent from NADPH to pteridine substrates. Early experiments using HPLC analyses to monitor the fate of tritium from (4*S*)-[^{3}H]NADPH during PTR1-catalyzed reduction of folate showed that most of the tritium appeared in THF, but small variable amounts also appeared in solvent water (data not shown). Control experiments indicated that this was likely due to nonenzymatic oxidation of [^{3}H]-NADPH, [^{3}H]THF, or both, during the reaction and/or HPLC analysis, but two precedents from related systems indicated a need for a more conclusive determination of the fate of the tritium. The NADH-dependent reduction of quinoid 7,8-dihydrobiopterin catalyzed by the mammalian enzyme DHPR (*36*, *37*) has been suggested to resemble the reduction of a flavin (*38*), in that the hydrogen transferred from NADH

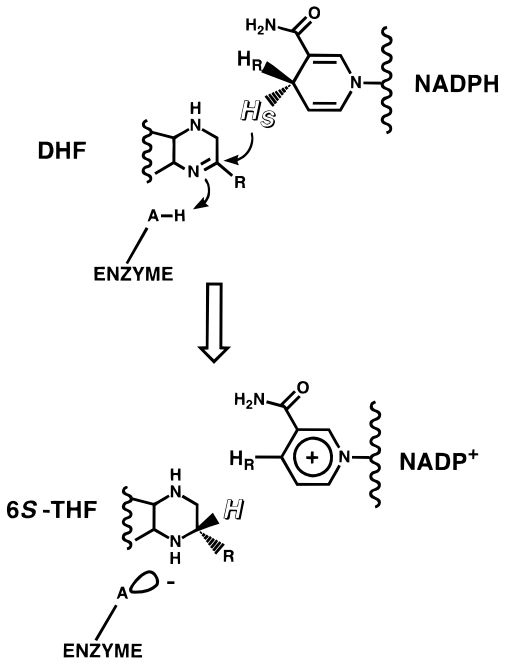

FIGURE 1: Stereochemistry of the PTR1-catalyzed reduction of DHF.

can be freely exchanged with solvent protons (*39*). Electrolytic or zinc metal reduction of fully oxidized pterins proceeds via a two-electron, two-proton process (*40*). The electrolytic process yields directly a 5,8-dihydropterin intermediate, which generally rearranges rapidly to a more stable 7,8-dihydropterin. It was also important to determine the stereochemistry at carbon 6 of the THF produced by PTR1-catalyzed reduction. A coupled enzyme system was used to settle both the site and stereochemistry of the PTR1-catalyzed hydrogen transfer to the pteridine.

Both the transfer of hydrogen from NADPH to carbon and the resulting stereochemistry were demonstrated by coupling PTR1 to TS, an enzyme known to utilize exclusively the 6*R* isomer of 5,10-methylene-5,6,7,8-THF (*24*−*26*). TS catalyzes the transfer of tritium from C6 of [6-^{3}H]methylene-THF to form the stable methyl group of dTMP. The stereoisomer of THF which corresponds to the 6*R* isomer of methylene-THF has *S* stereochemistry at carbon 6. Together, PTR1 and TS effectively catalyzed the time-dependent transfer of tritium from (4*S*)-[^{3}H]NADPH into dTMP. The conversion of [2-^{14}C]-2′-deoxyuridylate to [^{3}H,^{14}C]dTMP was 42, 61, and 100% complete at 30, 60, and 240 min under the conditions used; no dTMP was produced when either PTR1 or TS was omitted. Thus, PTR1-catalyzed reduction of the 5,6-double bond of DHF produces (6*S*)-THF, the isomer produced by DHFR (*26*). This result is consistent with the observation that expression of the PTR1 gene will permit the growth of an *E. coli* strain which is deficient in DHFR (Δ*fol*) on a medium lacking purines and methionine, for which the uncomplemented strain is auxotrophic (*41*). The 6*S* diastereoisomer of methylene-THF (formed from the 6*R* isomer of THF) is microbiologically inactive and incompetent as a substrate for several methylene-THF-dependent enzymes (*25*). Thus, the absolute stereochemistry of the hydride transfer to DHF catalyzed by PTR1 must be like that shown in Figure 1. [The possible identity of the enzymic acid shown in Figure 1 will be addressed in a future paper (J. Luba et al., manuscript in

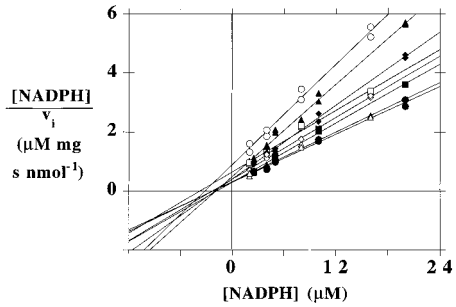

FIGURE 2: Dependence of the initial velocities of the PTR1-catalyzed NADPH-dependent reduction of folate upon substrate concentrations at pH 7 and 30 °C. The concentrations of folate were (●) 8 μM, (△) 6 μM, (■) 4 μM, (◇) 3 μM, (◆) 2 μM, (□) 1.5 μM, (▲) 1 μM, and (○) 0.75 μM.

preparation).] A similar result, indicating the "natural" stereochemistry at C6 of 5,6,7,8-tetrahydrobiopterin produced by PTR1-catalyzed reduction of biopterin, was previously demonstrated by the efficient coupling of the reactions catalyzed by PTR1 and phenylalanine hydroxylase (*5*).

Initial Velocity and Product Inhibition Patterns. The steady state kinetic analysis employed folate as the pteridine substrate. The rapid quench studies described below showed that DHF is an intermediate in the reduction of folate to THF. It would thus have been preferable to employ DHF, which only undergoes one reductive reaction, rather than folate, which undergoes two. However, the steady state kinetic analysis with DHF is complicated by the significant substrate inhibition seen with this pteridine (*5*). Folate was chosen instead of biopterin because the specific activity of PTR1 for folate was greater at neutral pH.[2]

When the initial velocities from varied NADPH at several fixed concentrations of folate (and vice versa) were analyzed by Hanes−Woolf plots, the lines intersected to the left of the *y*-axis (Figure 2). This indicates that catalysis by PTR1 proceeds via a ternary complex mechanism, as expected for a NADPH-dependent reductase which contains no apparent prosthetic group as an intermediate carrier of the reducing equivalents. No intersections at the origin were found in double-reciprocal (Lineweaver−Burke) plots of the data, either from varying NADPH at several fixed concentrations of folate or vice versa. Therefore, the kinetic mechanism of PTR1 is likely to be a steady state mechanism rather than an equilibrium mechanism. In the Hanes−Woolf plots, the *y*-intercepts of the lines are the reciprocals of the apparent values of V_{max}/K_M. The apparent V_{max}/K_M depends on the concentration of the fixed substrate, and the intersection of the lines defines the negative value of the dissociation constant of the substrate which binds first (*28*, *29*). We show below that NADPH binds first during the catalytic turnover of PTR1. Therefore, the intersection of the lines in Figure 2 occurs at $-K_d^{NADPH}$. Values for V_{max}, the K_Ms for both folate and NADPH, and the K_d for NADPH were determined from replots (Figure 3A,B) of the slopes and intercepts of the lines in Figure 2 (Table 1). The value of K_M for NADPH obtained in the absence of inhibitors (1.4 ± 0.2 μM) is about 10 times lower than values reported in earlier studies of PTR1 from *L. major* and *Leishmania tarentolae* (*5*, *6*). The higher values reported earlier may have been due to inhibition by a low-level $NADP^+$ contaminant ($K_i = 1 \pm 0.2$ μM) of the NADPH used and/or to the differing pHs employed in the previous studies.

[2] The specific activity of PTR1 for biopterin is highest at pH 4.6, where the nonenzymatic oxidation of NADPH would be a problem.

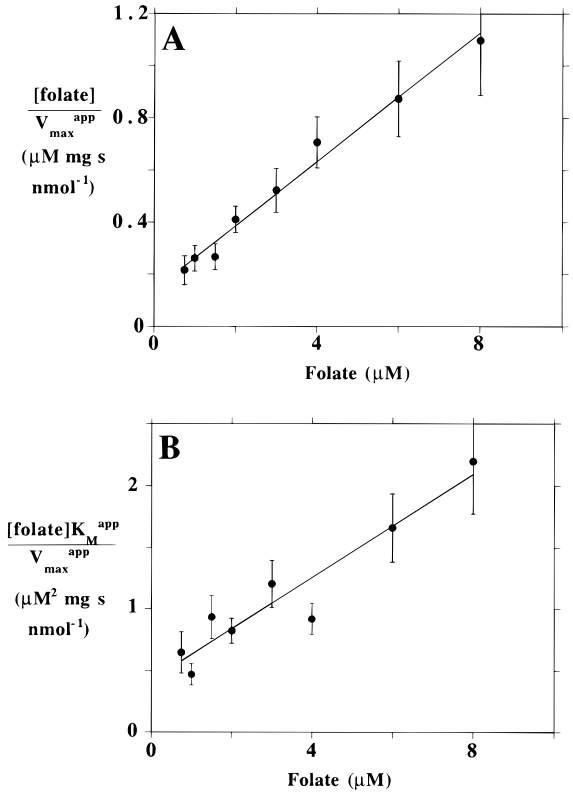

FIGURE 3: Secondary plots of the apparent steady state kinetic parameters (slopes and intercepts) from Figure 2. Standard errors of the slope and intercept values are indicated by the error bars. (A) A graph of $[folate]/V_{max}^{app}$ as a function of [folate]. The solid line indicates the theoretical fit of the data to eq 2. (B) A graph of $[folate]K_M^{app}/V_{max}^{app}$ as a function of [folate]. The solid line indicates the theoretical fit of the data to eq 3.

Table 1: Steady State Parameters of PTR1[a]

substrate	V_{max} (nmol mg^{-1} s^{-1})	k_{cat}/K_M[b] (μM^{-1} s^{-1})	K_M (μM)	K_d (μM)
NADPH	7.5 (±0.6)	0.16 (±0.04)	1.4 (±0.3)	3 (±1)[c] 0.46 (±0.02)[d]
folate	7.5 (±0.6)	0.26 (±0.06)	1.0 (±0.2)	*e*

[a] These values were measured at pH 7.0 and 30 °C. [b] Calculated from the V_{max}/K_M value with the indicated substrate using the molecular weight of the *L. major* PTR1 monomer (30 538 g/mol). [c] From the analysis of the steady state initial velocity data. [d] From the analysis of fluorescence intensity transfer data. [e] Does not bind to the apoenzyme.

Product inhibition patterns were employed to test the suspected order of substrate binding. The inhibition of PTR1 by the product $NADP^+$ is strictly competitive with NADPH (Figure 4A), indicating that NADPH and $NADP^+$ compete for the same form of the enzyme. The inhibition of PTR1 by the product $NADP^+$ is noncompetitive versus folate (Figure 4C). The inhibition by the product analogue 5dTHF was uncompetitive versus NADPH and noncompetitive versus folate (Figure 4B,D). The linear dependence of inhibition upon inhibitor concentration was observed in each case, and the results of the product inhibition studies are summarized in Table 2. These results are consistent with catalysis proceeding mainly via the ordered ternary complex

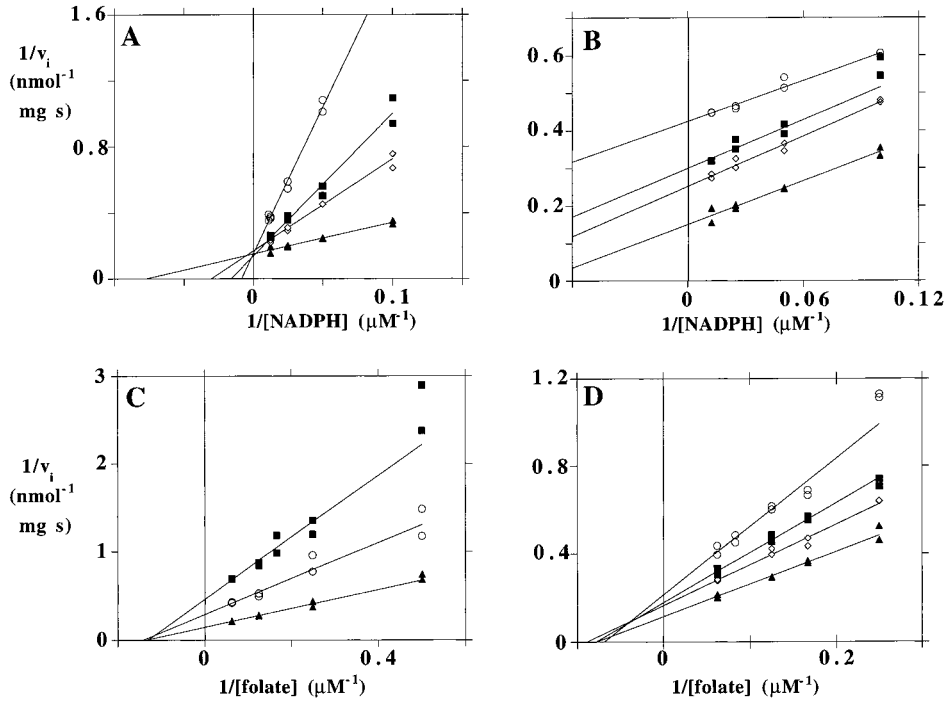

FIGURE 4: Effects of the product $NADP^+$ and of the product analogue 5dTHF upon the initial velocities (v_i) of PTR1-catalyzed reduction of folate (30 μM) by NADPH. Double-reciprocal plots are shown at several fixed concentrations of product or product analogue. When folate was varied, NADPH was held at 90 μM. When NADPH was varied, folate was held at 16 μM. Regression of the data upon the appropriate equation (eq 4, 5, or 6) provided estimates of the K_i values in each case. The solid lines represent the theoretical curves at the various inhibitor concentrations, calculated using the optimized parameters listed in Tables 1 and 2. (A) Initial velocities of the PTR1-catalyzed reduction of folate at fixed folate, varied NADPH, and several fixed concentrations of $NADP^+$. The $NADP^+$ concentrations were (▲) 0 μM, (◇) 2.5 μM, (■) 5 μM, and (○) 10 μM. (B) Initial velocities of the PTR1-catalyzed reduction of folate at fixed folate, varied NADPH, and several fixed concentrations of 5dTHF. The 5dTHF concentrations were (▲) 0 μM, (◇) 20 μM, (■) 40 μM, and (○) 80 μM. (C) Initial velocities of the PTR1-catalyzed reduction of folate at fixed NADPH, varied folate, and several fixed concentrations of $NADP^+$. The concentrations of $NADP^+$ were (▲) 0 μM, (○) 1 μM, and (■) 2.5 μM. (D) Initial velocities of the PTR1-catalyzed reduction of folate at fixed NADPH, varied folate, and several fixed concentrations of 5dTHF. The 5dTHF concentrations were (▲) 0 μM, (◇) 10 μM, (■) 20 μM, and (○) 40 μM.

Table 2: Patterns of Product Inhibition of PTR1-Catalyzed Reduction of Folate by NADPH

varied substrate	inhibitor[a]	mode of inhibition[b]	K_i (μM)[c]
NADPH	$NADP^+$	C	1 (±0.2)
NADPH	5dTHF	U	39 (±6)
folate	$NADP^+$	N	1.06 (±0.08)
folate	5dTHF	N	41 (±12)

[a] Because of the instability of THF, the product analogue 5dTHF was used. [b] The modes of inhibition were as follows: C, competitive; U, uncompetitive; and N, noncompetitive. [c] Calculated from the data in Figure 4A−D.

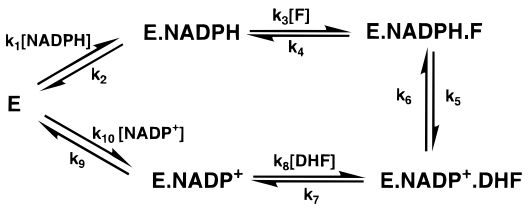

FIGURE 5: Kinetic mechanism of PTR1.

pathway shown in Figure 5, with binding of NADPH preceding that of the oxidized pteridine substrate, and dissociation of the reduced pteridine product preceding that of $NADP^+$. The fact that 5dTHF acts as a noncompetitive inhibitor versus folate suggests that 5dTHF binds to both the enzyme−NADPH and the enzyme−$NADP^+$ complexes. If 5dTHF were unable to bind to the enzyme−NADPH complex, the observed inhibition versus folate would have been uncompetitive.

Ligand Binding. The enhanced fluorescence of NADPH at 450 nm upon excitation at 295 nm in the presence of PTR1 presumably arises from energy transfer between the enzyme and bound NADPH (Figure 6A). The fluorescence of the bound NADPH is quenched upon addition of methotrexate (data not shown). Addition of DHF (Figure 7) quenched the intrinsic tryptophan fluorescence of the apoenzyme. Although the enzyme's fluorescence also was decreased upon addition of folate or methotrexate to solutions containing PTR1 alone, most or all of these decreases were due to absorbance. Folate and methotrexate each absorb more strongly at 340 nm than does DHF. The effects of folate or methotrexate on the intensity of PTR1's fluorescence intensity was nearly identical to their effects on the fluorescence of pure tryptophan. These results suggest either that the affinities of folate and methotrexate for PTR1 alone are much lower than that of DHF or that formation of either a PTR1−folate complex or a PTR1−methotrexate complex does not much alter the enzyme's fluorescence. The former hypothesis seems more likely, given the quenching by DHF with the apoenzyme and by methotrexate with the enzyme−NADPH complex.

The linear dependence of the NADPH-dependent fluorescence intensity observed at subsaturating NADPH concentrations in the presence of 5 μM PTR1 (Figure 6B) indicated that NADPH must bind with a dissociation constant (K_d) of

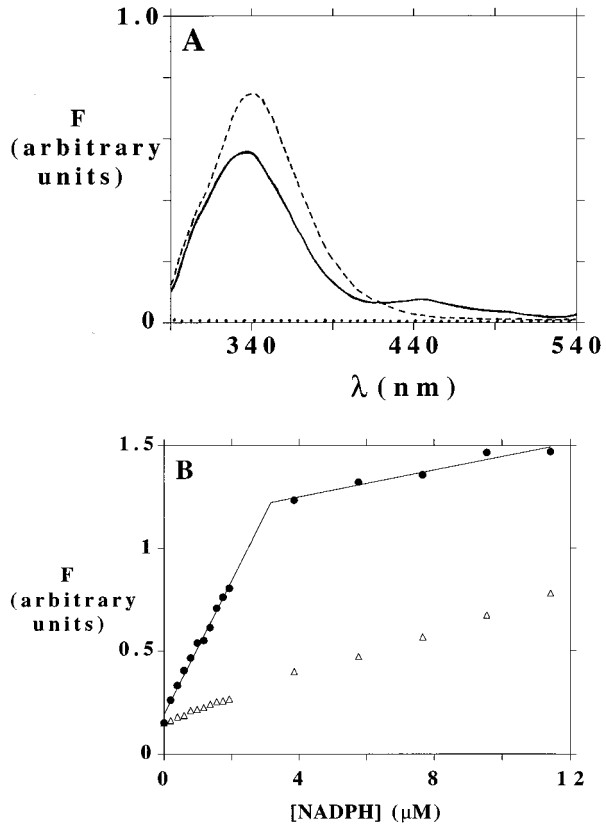

FIGURE 6: (A) Fluorescence emission spectra of solutions containing *L. major* PTR1 (5 μM, dashed line), NADPH (5 μM, dotted line), or both (solid line). Excitations were done with a 5 nm band of radiation centered at 295 nm; the emission slit was also 5 nm. (B) The increases in fluorescence intensity (*F*) at 450 nm were used to analyze NADPH binding to PTR1. The open triangles show the data for NADPH alone. These measurements were made at a higher detector sensitivity than the spectra shown in panel A. The data measured in the presence of 5 μM PTR1 (solid circles) above and below 4 μM NADPH were fit to separate straight lines, intersecting at 3.2 μM.

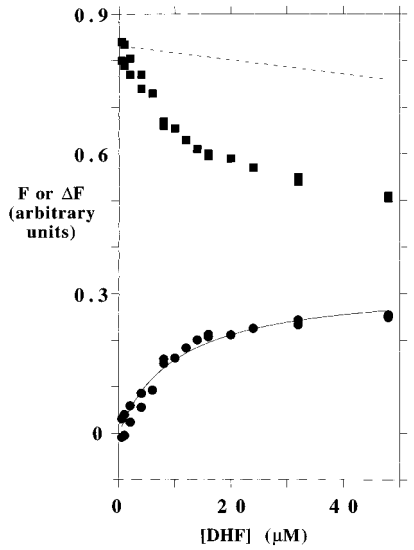

FIGURE 7: Quenching of PTR1 fluorescence by DHF. Excitation and emission wavelengths were 290 and 340 nm, respectively. The reduction of emission intensity due to absorbance by DHF at 340 nm (broken line), quantitated using a solution of 7.5 μM tryptophan, was linear over this concentration range. Values for the observed fluorescence (*F*) of a 5 μM solution of PTR1 (■) were subtracted from this line. These differences (ΔF, ○) were fit by nonlinear least-squares regression of the data to eq 7, yielding a K_d of 10 ($\pm$1.6) μM. The solid line shows the theoretical curve for this fit.

$\ll$5 μM. The value of K_d was determined to be 0.46 ($\pm$0.02) μM from a quantitative analysis of the fluorescence enhancement observed using 0.5 μM PTR1. The K_d estimated in the fluorescence titration is significantly lower than the rather poorly defined value (3 $\pm$ 1 μM) estimated from the steady state kinetic analysis. However, these values are in much better agreement than either is with the K_d value of 130 μM recently reported for PTR1 from *L. tarentolae* (*6*). The source of the discrepancy between the value reported here and the value reported by Wang and co-workers is unclear. A K_d of 130 μM for NADPH is much higher than has been observed with other SDRs and is more than 7-fold higher than the K_M for NADPH (17 μM) reported by the same workers (*6*). The discrepancy may be related to the fact that *L. tarentolae* PTR1 was obtained from a MalE fusion protein and may have suffered from structural alterations during cleavage. Alternatively, this discrepancy may simply reflect difficulties with the interpretation of fluorescence data as has been previously noted for binding of NADH to DHPR (*37*).

The two intersecting lines shown in Figure 6B describe the fluorescence of NADPH upon binding to PTR1 and of excess NADPH. The intersection of the two lines (at 3.2 μM) provides an estimate of the PTR1 active sites available for NADPH binding in the 5 μM protein solution. Values of the ratio between the concentration of binding sites and the protein concentration, from this and other titrations, were consistently 0.5 $\pm$ 0.1. The possible significance of the substoichiometric ratio is discussed below.

The apparent K_d for DHF binding to the free enzyme, derived by fitting the fluorescence quenching data shown in Figure 7 to eq 7, is 10 ($\pm$2) μM. Since the steady state kinetics presented above and the isotope partitioning results discussed below indicate that the enzyme−NADPH complex is the only productive binary complex, the PTR1−DHF complex lies off the reaction pathway. The K_d for DHF binding to the free enzyme is very close to the K_i for substrate inhibition by DHF (*5*). The nonproductive PTR1−DHF complex may in part be responsible for that inhibition.

Isotope Partitioning. The steady state kinetic results are consistent with an ordered ternary complex mechanism. In this model, NADPH must bind to PTR1 first, followed by binding of the pteridine substrate. After both substrates are bound, the redox chemistry ensues, the reduced pteridine dissociates from the ternary complex of enzyme and products, and $NADP^+$ dissociates last (Figure 5). However, with DHF at least, the data from fluorescence quenching indicate that pteridine binding to PTR1 may occur without NADPH binding. It was therefore important to test whether such a binary PTR1−pteridine complex could be catalytically competent. The partitioning approach developed by Rose and associates ["isotope trapping" (*42*, *43*)] was employed to make this determination.

Treatment of a mixture of [^{14}C]NADPH and PTR1 (5 μM each) with 40 μM DHF and a 200-fold molar excess of nonradioactive NADPH resulted in the conversion of about half (mean of four independent experiments, 46%; standard deviation, 13%) of the [^{14}C]NADPH to $NADP^+$ (Figure 8). An insignificant amount of radioactive $NADP^+$ was formed

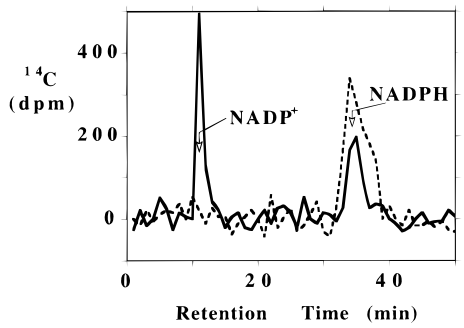

FIGURE 8: Analysis of the partitioning of the [^{14}C]NADPH−PTR1 complex. A sample containing [^{14}C]NADPH and PTR1 (5 μM each) was mixed manually with an equal volume of 80 μM DHF and 2 mM nonradioactive NADPH. After 12 s, the reaction was quenched by addition of methotrexate. Protein was removed from the reaction mixture, and a sample was analyzed by HPLC and liquid scintillation counting (solid line) as described in Materials and Methods. The dashed line shows a similar analysis with a sample in which the [^{14}C]NADPH was mixed with the enzyme simultaneously with the DHF and nonradioactive NADPH.

when the [^{14}C]NADPH was added to PTR1 at the same time as the DHF and nonradioactive NADPH. Similar results were obtained when 100 μM DHF was used as the trap or when DHF was replaced by folate (100 μM). In contrast with these results, [^{3}H]folate or [^{3}H]DHF premixed with PTR1 was not trapped upon the addition of the mixture to NADPH and excess nonlabeled pteridine substrate. On the single-turnover time scale, significant conversion of [^{3}H]-folate or [^{3}H]DHF to reduced radioactive products only occurred when the enzyme/pteridine mixture was added to NADPH in the absence of nonradioactive folate or DHF.

The results of the partitioning experiments show that a significant fraction of the enzyme−NADPH complex is catalytically competent, but enzyme−pteridine binary complexes probably are not. These results are consistent with obligatory binding of NADPH to PTR1 prior to pteridine binding for a catalytically productive ternary complex. They are inconsistent with a random mechanism in which either NADPH or pteridine can bind first. Saturating concentrations of folate or DHF trapped only half of the PTR1−NADPH complex, rather than all of it. In control experiments with [^{14}C]NADPH, all of this substrate was capable of being converted to product. The fraction of [^{14}C]NADPH trapped was essentially identical at 40 or 100 μM DHF, or at 100 μM folate, concentrations which are much higher than the K_M values for these substrates. Moreover, doubling the concentration of PTR1 did not increase the fraction of [^{14}C]-NADPH trapped. This may indicate that only about half of the enzyme−NADPH binary complex is catalytically competent. It is noteworthy that the fraction of active sites seen by fluorescence titration of PTR1 with NADPH (0.5 ± 0.1) is similar to the fraction of the PTR1−[^{14}C]NADPH complex which could be trapped.

Kinetic Isotope Effects. The use an isotope effect to test the kinetic mechanism for PTR1 was appealing because this approach is insensitive to the existence of nonproductive complexes and yields information complementary to that provided by the product inhibition patterns and isotope partitioning methods. The product recycling method which we devised to maintain constant concentrations of the second substrate allowed substantial amounts of the product to be formed from the first substrate, at either low or high levels of the second substrate, without the need to make multiple additions as the reaction proceeds. This approach should be generally applicable to other competitive isotope effect measurements, where the appropriate chemical or enzymatic systems exist to allow product recycling.

Table 3: Measurement of $^T(V/K)$ of the PTR1-Catalyzed Reduction of DHF[a]

[DHF] (μM)	R_0[b] (Ci/mol)	R_s[b] (Ci/mol)	f[c]	$^T(V/K)$
0.5	11.9 (±0.5)	13.5 (±0.4)	0.24 (±0.03)	1.8
0.5	13.95 (±0.15)	15.0 (±0.3)	0.23 (±0.009)	1.3
0.5	12.75 (±0.15)	15.1 (±0.2)	0.27 (±0.005)	2.1
60	18.75 (±0.35)	19.35 (±0.35)	0.62 (±0.01)	1.04
60	9.0 (±0.2)	9.7 (±0.2)	0.841 (±0.007)	1.04

[a] The definitions of R_0, R_s, and f are given in Materials and Methods. Measurements were made at pH 7.5 and 30 °C. [b] Represents the mean of seven determinations. [c] Represents the mean of three to five determinations.

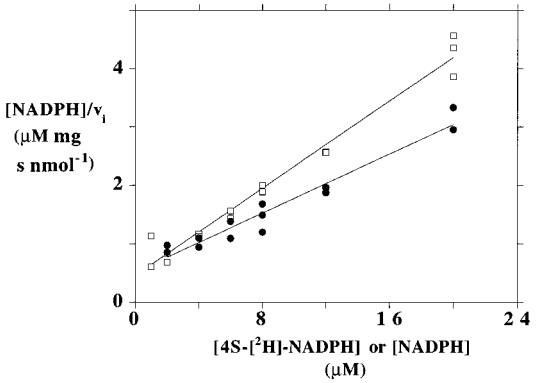

FIGURE 9: Deuterium isotope effects on the PTR1-catalyzed reduction of folate. The data were collected at pH 6.0 and 30 °C using the spectrophotometric assay described in Materials and Methods. The open squares and solid circles represent the data obtained with deuterium-substituted and unsubstituted NADPH, respectively. The solid lines are the theoretical fits of the data in each case to eq 8. The optimized values of the kinetic parameters, V_{max} and V_{max}/K_{MN}, were 7.9 (±0.6) nmol mg^{-1} s^{-1} and 1.9 (±0.3) nmol mg^{-1} s^{-1} μM^{-1} for unsubstituted NADPH and 5.4 (±0.2) nmol mg^{-1} s^{-1} and 2.2 (±0.4) nmol mg^{-1} s^{-1} μM^{-1} for 4-deuterium-substituted NADPH, respectively.

At subsaturating DHF, a significant tritium effect [$^T(V/K) = 1.8 \pm 0.4$] for the PTR1-catalyzed reduction of DHF was observed (Table 3). At saturating DHF, the value of $^T(V/K)$ was near unity. It is important to note that the experimental conditions were designed to ensure that all 5,10-methylene-THF produced was rapidly and quantitatively converted back to DHF so that the substantial isotope effect on the reaction catalyzed by TS (*44*) would not interfere with the measurement of $^T(V/K)$ on the PTR1-catalyzed reaction. The fact that high concentrations of the second substrate reduce the observed value of $^T(V/K)$ to unity indicates strongly that PTR1 is governed by a steady state ordered ternary complex mechanism (*33*). The observed isotope effect for an equilibrium ordered kinetic mechanism should be independent of the concentration of the second substrate.

A value of 1.6 (±0.2) was measured for ^DV for folate (Figure 9), arising from the deuterium substitution of the *pro-S* hydrogen at C4 of NADPH. This is probably too low to be the intrinsic effect and indicates that the rate of conversion of the ternary enzyme−NADPH−pteridine complex to product is only partially limited by the chemistry of

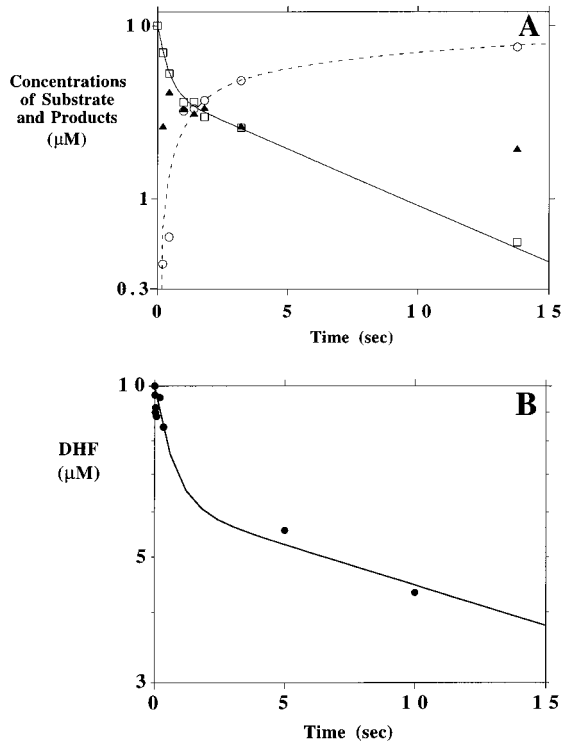

FIGURE 10: Rapid quench kinetic analysis of PTR1-catalyzed reduction of (A) folate and (B) DHF. The concentrations of PTR1 and NADPH were 80 and 0.5 μM, respectively. (A) The theoretical curve for the disappearance of folate is a sum of two exponentials with time constants of 3 and 0.15 s^{-1} and approximately equal amplitudes (59 and 41% for the rapid and slow phases, respectively). The symbols are (□) [folate], (▲) [DHF], and (○) [THF] at a given time point. The theoretical curve for the appearance of THF is a sum of two exponentials with time constants of 0.8 and 0.07 s^{-1} and amplitudes of 39 and 61% for the rapid and slow phases, respectively. (B) The theoretical curves for the disappearance of DHF (and appearance of THF, not shown) are each a sum of two exponentials with time constants of 1.5 and 0.03 s^{-1} and amplitudes of 38 and 62% for the rapid and slow phases, respectively. The solid circles represent [DHF] at a given time point.

hydride transfer. The turnover rate must also be partially determined by other steps. The value of $^{D}(V/K)$ is indistinguishable from unity (0.9 ± 0.2) as expected since the parameter was measured at 30 μM folate which saturated the enzyme with the second substrate.

Pre-Steady State Kinetics. The reduction of 10 μM folate by an excess of the PTR1−NADPH complex (80 μM) was accompanied by the transient appearance of DHF (Figure 10A). This is a direct demonstration that DHF is an intermediate in the conversion of folate to THF. Surprisingly, the time course for the conversion of folate to THF was not well described by monophasic kinetics, but was rather well described by biphasic kinetics. The theoretical curve shown in Figure 10A for disappearance of folate is the sum of two exponentials. The two processes have apparent rate constants of 3 and 0.15 s^{-1} and approximately equal amplitudes (59 and 41% for the rapid and slow phases, respectively). Note that these pseudo-first-order rate constants are not comparable to turnover numbers, since these studies were carried out under conditions of excess enzyme, but they can be compared to the encounter constants (vide infra). The time course of THF appearance was also poorly described by a single exponential (Figure 10A). Similar results were obtained using 10 μM folate and 37 μM PTR1−NADPH (data not shown), with rate constants that were about half the values obtained using 80 μM enzyme. At both enzyme concentrations, DHF was formed from folate and disappeared on a time scale consistent with its competence as a kinetic intermediate. The reduction of 10 μM DHF by an excess of the PTR1−NADPH complex also occurred with biphasic kinetics (Figure 10B), with rapid and slow phases (rate constants of 1.5 and 0.03 s^{-1}, respectively) of similar amplitudes (38 and 62%, respectively).

We interpret the biphasic kinetics for reduction of folate or DHF by excess PTR1 as being consistent with the existence of two forms of the enzyme−NADPH complex. Since all of the pteridine substrate was sequestered, with approximately half reduced slowly despite the presence of a large excess of enzyme, both forms of the enzyme−NADPH complex must bind to folate (or DHF) with nearly equal avidity. This idea is consistent with the fact that only about half of the PTR1−NADPH complex could be trapped in the isotope partitioning experiments. The steady state kinetics are dominated by the rapidly reacting forms of the enzyme−NADPH complex. The apparent second-order rate constants for the faster phases of folate and DHF reduction (assuming that only half of the enzyme present participates in this phase) are 0.1 (±0.02) and 0.04 (±0.02) μM^{-1} s^{-1}, respectively. These values are comparable to the values of $k_{cat}/K_{M,folate}$ obtained from the steady state kinetics (0.26 and 0.06 μM^{-1} s^{-1}, respectively).

Comparison of PTR1, SDRs, and DHFR. The stereochemical course and kinetic mechanism of PTR1 are very similar to those which have been described for many members of the SDR family. The preference of PTR1 for transfer of the *pro-S* hydrogen from NADPH is observed for all other members of the SDR family which have been studied (*39*, *45*−*51*). Members of the AKR family (*9*) have been observed, like DHFR, to transfer the A-side hydrogen of NADH or NADPH (*52*−*55*). This stereochemical result, therefore, resolves the ambiguity regarding whether PTR1 is a member of the SDR family or the AKR family. Amino acid sequence comparisons (*2*, *3*) indicated that PTR1 belongs to a superfamily of oxidoreductases, but sequence comparisons alone have been shown to be insufficient to assign a protein to the AKR or SDR families. For example, the presence of the Tyr-$(Xaa)_3$-Lys motif is considered to be diagnostic of the SDRs. However, several proteins with the SDR fold lack this motif in their primary sequences (*56*, *57*), and two AKRs each have a Tyr-$(Xaa)_3$-Lys sequence in a surface site distant from the catalytic cleft (*58*−*60*). The steady state ordered ternary complex kinetic mechanism for PTR1 (Figure 5) is analogous to mechanisms reported for both SDRs [such as *Drosophila* alcohol dehydrogenase (*61*) and DHPR (*62*)] and AKRs [such as aldose reductase (ref *63* and references therein)]. Results with several site-directed mutant forms of PTR1 (*41*) further support structural homology between PTR1 and other SDRs.

DHPR, a mammalian member of the SDR family, is unusual in that it requires a non-ground state substrate, quinoid dihydrobiopterin. Since the π electron structure of quinoid dihydrobiopterin resembles the structure found in oxidized flavins, the mechanism of DHPR catalysis has been suggested to resemble the reduction of flavin observed in flavoproteins (*38*) such as glutathione reductase (*64*). This is supported by the release of ^{3}H into solution when (4*S*)-

[^{3}H]NADH is oxidized by DHPR (*39*). In contrast to DHPR, PTR1 does not utilize quinoid dihydrobiopterin as a substrate (*4*, *6*). The hydride transfer mechanism used by PTR1 and the reduction of ground state substrates resemble catalysis by DHFR, despite the fact that PTR1 is likely to be structurally homologous to DHPR and not to DHFR. DHFR has no apparent structural similarity with respect to either the AKRs or the SDRs. Most SDRs transfer hydride directly to (from) the carbon of a carbonyl (alcohol) moiety.

A complex kinetic mechanism has been observed for DHFR (*65*). Either NADPH or DHF may bind to DHFR first in the progression to a catalytically competent ternary complex, and the products may dissociate in either order. However, the most rapid pathway during steady state turnover (and therefore the catalytic circuit of highest conductance) is one in which NADPH binds not only prior to DHF but also before dissociation of the THF produced from the previous turnover. Rapid dissociation of the THF product requires dissociation of $NADP^+$ and binding of a fresh molecule of NADPH. In contrast to DHFR, PTR1 must bind to NADPH first and likely releases $NADP^+$ after the release of the reduced pteridine. As in the case of DHPR (*15*), the creation of functional enzyme requires that PTR1 bind to NADPH, but unlike DHPR, a binding site on PTR1 for at least one pteridine substrate (DHF) exists in the absence of NADPH.

Several pieces of evidence seem to indicate that two forms of the PTR1−NADPH binary complex exist. Trapping of the PTR1−[^{14}C]NADPH complex by folate or DHF results in the oxidation of only about half of the radiolabeled NADPH to product. The stoichiometry of NADPH binding sites shown by fluorescence enhancement with PTR1 was 0.5 (±0.1); another population of sites could be present which was not made evident by this method. Finally, the biphasic kinetics of folate or DHF reduction by excess PTR1−NADPH are also consistent with the existence of at least two forms of this binary complex. The physical meaning and physiological relevance of this "half-of-the-sites" behavior is not clear. Those SDRs whose crystallographic structures are known have one active site per subunit, distinct from the subunit−subunit contact surfaces. PTR1 has been shown to exist as a tetramer in solution (*5*, *6*), like many other SDRs. Although no steady state kinetic evidence for either positive or negative cooperativity was observed, each subunit in the PTR1 tetramer may respond allosterically to the status of the other subunits. Perhaps that form of the PTR1−NADPH complex which does not turn over rapidly must undergo a slow structural rearrangement to allow catalysis, or perhaps this form is a slowly dissociating dead-end complex. The available data do not distinguish between these possibilities. We are not aware of any reports of similar behavior by other SDRs. In particular, isotope trapping experiments with the DHPR−NADH binary complex demonstrated stoichiometric conversion of that complex to NAD^+ by saturating quinoid dihydrobiopterin (*62*).

A conformational change has been postulated to limit at least partially the rate of catalysis by DHPR (*62*). The crystal structures of the binary and ternary complexes of 7α-hydroxysteroid dehydrogenase show that large conformational changes occur upon substrate binding to the enzyme−NADPH complex (*14*). Given the low magnitude of ^DV for PTR1-catalyzed reduction of folate, a conformational change and/or product release step may also be largely rate-determining for catalysis by PTR1.

PTR1 differs significantly in both mechanism and primary structure from DHPR and DHFR. These unique features of PTR1 may make this enzyme vulnerable to selective inhibition, a desirable goal for the development of antifolate therapeutics for treatment of leishmaniasis (*8*).

ACKNOWLEDGMENT

The contents of this paper represent solely the views of the authors and are not necessarily those of the U.S. Public Health Service. We thank Ms. E. Nalivaika for a sample of thymidylate synthase, Dr. C. J. Shih of Eli Lilly for a gift of 5-deazatetrahydrofolate, Professor W. Pfleiderer for a helpful discussion regarding the electrolytic reduction of pterins, and anonymous reviewers of an earlier version of the manuscript for their helpful criticisms.

REFERENCES

1. Beverley, S. M., Coderre, J. A., Santi, D. V., and Schimke, R. T. (1984) *Cell 38*, 431−439.
2. Callahan, H. L., and Beverley, S. M. (1992) *J. Biol. Chem. 267*, 24165−24168.
3. Papadopoulou, B., Roy, G., and Ouellette, M. (1992) *EMBO J. 11*, 3601−3608.
4. Bello, A. R., Nare, B., Freedman, D., Hardy, L., and Beverley, S. M. (1994) *Proc. Natl. Acad. Sci. U.S.A. 91*, 11442−11446.
5. Nare, B., Hardy, L. W., and Beverley, S. M. (1997) *J. Biol. Chem. 272*, 11883−11891.
6. Wang, J., Leblanc, E., Chang, C.-F., Papadopoulou, B., Bray, T., Whiteley, J. M., Lin, S.-X., and Ouellette, M. (1997) *Arch. Biochem. Biophys. 342*, 197−202.
7. Hardy, L. W., Matthews, W., Nare, B., and Beverley, S. M. (1997) *Exp. Parasitol. 114*, S101−S110.
8. Nare, B., Luba, J., Hardy, L. W., and Beverley, S. M. (1997) *Parasitology 114*, S101−S110.
9. Bruce, N. C., Willey, D. L., Coulson, A. F. W., and Jeffery, J. (1994) *Biochem. J. 299*, 805−811.
10. Jornvall, H., Persson, B., Krook, M., Arian, S., Gonzalez-Duarte, R., Jeffery, J., and Ghosh, D. (1995) *Biochemistry 34*, 6003−6013.
11. Su, Y., Varughese, K. I., Xuong, N. H., Bray, T. L., Roche, D. J., and Whiteley, J. M. (1993) *J. Biol. Chem. 268*, 26836−26841.
12. Ghosh, D., Wawrzak, Z., Weeks, C. M., Duax, W. L., and Erman, M. (1994) *Structure 2*, 629−640.
13. Tanaka, N., Nonaka, T., Nakanishi, M., Deyashiki, Y., Hara, A., and Mitsui, Y. (1996) *Structure 4*, 33−45.
14. Tanaka, N., Takamasa, N., Tanabe, T., Yoshimoto, T., Tsuru, D., and Mitsui, Y. (1996) *Biochemistry 35*, 7715−7730.
15. Kiefer, P. M., Varughese, K. I., Su, Y., Xuong, N.-H., Chang, C.-F., Gupta, P., Bray, T., and Whiteley, J. M. (1996) *J. Biol. Chem. 271*, 3437−3444.
16. Little, J. W. (1972) *Anal. Biochem. 48*, 217−224.
17. Reddy, S. R., Sacchetini, J. C., and Blanchard, J. S. (1995) *Biochemistry 34*, 3492−3501.
18. Lowenstein, J. M. (1961) *J. Biol. Chem. 236*, 1213.
19. Wang, T. P., Kaplan, N. O., and Stolzenbach, F. E. (1954) *J. Biol. Chem. 211*, 465−472.
20. Jeong, S. S., and Gready, J. E. (1994) *Anal. Biochem. 221*, 273−277.
21. Futterman, S. (1957) *J. Biol. Chem. 228*, 1031−1036.
22. Hardy, L. W., and Nalivaika, E. (1992) *Proc. Natl. Acad. Sci. U.S.A. 89*, 9725−9729.
23. Baccanari, D., Smith, P. S., Sinski, D., and Burchall, J. (1975) *Biochemistry 14*, 5267−5273.
24. Blakley, R. L. (1969) *The Biochemistry of Folic Acid and Related Pteridines*, Wiley, New York.
25. Kaufman, B. T., Donaldson, K. O., and Keresztesy, J. C. (1963) *J. Biol. Chem. 238*, 1498−1500.

26. Fontecilla-Camps, J., Bugg, C. E., Temple, C., Rose, J. D., Montgomery, J. A., and Kisliuk, R. L. (1979) *J. Am. Chem. Soc. 101*, 6114−6115.
27. Bradford, M. M. (1976) *Anal. Biochem. 72*, 248−254.
28. Cleland, W. W. (1963) *Biochim. Biophys. Acta 67*, 104−137.
29. Cornish-Bowden, A. (1995) *Fundamentals of Enzyme Kinetics*, Portland Press, London, U.K.
30. Cleland, W. W. (1963) *Biochim. Biophys. Acta 67*, 173−187.
31. Janin, J., van Rapenbusch, R., Truffa-Bachi, P., and Cohen, G. N. (1969) *Eur. J. Biochem. 8*, 128−138.
32. Northrop, D. B. (1977) *Isotope Effects on Enzyme-Catalyzed Reactions*, University Park Press, Baltimore.
33. Cook, P. F., and Cleland, W. W. (1981) *Biochemistry 20*, 1790−1796.
34. Blakley, R. L., Ramasastri, B. V., and McDougall, B. M. (1963) *J. Biol. Chem. 238*, 3075−3079.
35. Pastore, E. J., and Friedkin, M. (1962) *J. Biol. Chem. 237*, 3802−3810.
36. Kaufman, S. (1963) *Proc. Natl. Acad. Sci. U.S.A. 50*, 1085−1093.
37. Shiman, R. (1985) in *Folates and Pterins* (Blakley, R. L., and Benkovic, S. J., Eds.) Vol. 2, pp 179−249, John Wiley & Sons, Inc., New York.
38. Whiteley, J. M., Xuong, N. H., and Varughese, K. I. (1993) *Adv. Exp. Med. Biol. 338*, 115−121.
39. Armarego, W. L. (1979) *Biochem. Biophys. Res. Commun. 89*, 246−249.
40. Kwee, S., and Lund, H. (1973) *Biochim. Biophys. Acta 297*, 285−296.
41. Luba, J. (1997) Ph.D. Dissertation, University of Massachusetts Graduate School of Biomedical Sciences, Worcester, MA.
42. Rose, I. A., O'Connell, E. L., and Litwin, S. (1974) *J. Biol. Chem. 249*, 5163−5168.
43. Rose, I. A. (1980) *Methods Enzymol. 64*, 47−59.
44. Spencer, T., Villafranca, J. E., and Appleman, J. R. (1997) *Biochemistry 36*, 4212−4222.
45. Alizade, M. A., Gaede, K., and Brendel, K. (1976) *Hoppe-Seyler's Z. Physiol. Chem. 357*, 1163−1169.
46. Arnold, L. J., Jr., You, K., Allison, W. S., and Kaplan, N. O. (1976) *Biochemistry 15*, 4844−4849.
47. Benner, S. A., Nambian, K. P., and Chambers, G. K. (1985) *J. Am. Chem. Soc. 107*, 5513−5517.
48. Betz, G., and Warren, J. C. (1968) *Arch. Biochem. Biophys. 128*, 745−752.
49. Do Nascimento, K. H., and Davies, D. D. (1975) *Biochem. J. 149*, 553−557.
50. Jarabak, J., and Talalay, P. (1960) *J. Biol. Chem. 235*, 2147−2151.
51. Nakayama, T., and Sawada, H. (1986) *Biochim. Biophys. Acta 882*, 220−227.
52. Deyashiki, Y., Ohshima, K., Nakanishi, M., Sato, K., Matsuura, K., and Hara, A. (1995) *J. Biol. Chem. 270*, 10461−10467.
53. Feldman, H. B., Szczepanik, P. A., Havre, P., Corrall, R. J. M., Yu, L. C., Rodman, H. M., Rosner, B. A., Klein, P. D., and Landau, B. R. (1977) *Biochim. Biophys. Acta 480*, 14−20.
54. Flynn, T. G., Shires, J., and Walton, D. J. (1975) *J. Biol. Chem. 250*, 2933−2940.
55. Pineda, J. A., Murdock, G. L., Watson, R. J., and Warren, J. C. (1989) *J. Steroid Biochem. 33*, 1223−1228.
56. Dessen, A., Quemard, A., Blanchard, J. S., Jacobs, W. R., Jr., and Sacchettini, J. S. (1995) *Science 267*, 1638−1641.
57. Rafferty, J. B., Simon, J. W., Baldock, C., Artymiuk, P. J., Baker, P. J., Stuitje, A. R., Slabas, A. R., and Rice, D. W. (1995) *Structure 3*, 927−938.
58. Borhani, D. W., Harter, T. M., and Petrash, J. M. (1992) *J. Biol. Chem. 267*, 24841−24847.
59. Wilson, D. K., Bohren, K. M., Gabbay, K. H., and Quiocho, F. A. (1992) *Science 257*, 81−84.
60. Hoog, S. S., Pawlowski, J. E., Alzari, P. M., Penning, T. M., and Lewis, M. (1994) *Proc. Natl. Acad. Sci. U.S.A. 91*, 2517−2521.
61. Winberg, J. O., and J. S. McKinley-McKee, J. S. (1994) *Biochem. J. 301*, 901−909.
62. Poddar, S., and Henkin, J. (1984) *Biochemistry 23*, 3143−3148.
63. Grimshaw, C. E., Bohren, K. M., Lai, C.-J., and Gabbay, K. H. (1995) *Biochemistry 34*, 14356−14365.
64. Pai, E., and Schulz, G. (1983) *J. Biol. Chem. 258*, 1752−1757.
65. Fierke, C. A., Johnson, K. A., and Benkovic, S. J. (1987) *Biochemistry 26*, 4085−4092.
66. Su, Y., Varughese, K. I., Xuong, Ng. H., Bray, T. L., Roche, D. J., and Whiteley, J. M. (1993) *J. Biol. Chem. 268*, 26836−26841.

BI972693A